

**NASA  
Technical  
Memorandum**

NASA TM - 108419

1N-26  
185538  
29P  
453369

(NASA-TM-108419) MICROSTRUCTURAL  
EVOLUTION OF NARLOY-Z AT ELEVATED  
TEMPERATURES (NASA) 29 p

N94-13715

Unclas

G3/26 0185538

**MICROSTRUCTURAL EVOLUTION OF NARLOY-Z  
AT ELEVATED TEMPERATURES**

By J. Singh, G. Jerman, B.N. Bhat, and R. Poorman

Materials and Processes Laboratory  
Science and Engineering Directorate

September 1993



National Aeronautics and  
Space Administration

George C. Marshall Space Flight Center

# REPORT DOCUMENTATION PAGE

Form Approved  
OMB No. 0704-0188

Public reporting burden for this collection of information is estimated to average 1 hour per response, including the time for reviewing instructions, searching existing data sources, gathering and maintaining the data needed, and completing and reviewing the collection of information. Send comments regarding this burden estimate or any other aspect of this collection of information, including suggestions for reducing this burden, to Washington Headquarters Services, Directorate for Information Operations and Reports, 1215 Jefferson Davis Highway, Suite 1204, Arlington, VA 22202-4302, and to the Office of Management and Budget, Paperwork Reduction Project (0704-0188), Washington, DC 20503.

<b>1. AGENCY USE ONLY (Leave blank)</b>	<b>2. REPORT DATE</b> September 1993	<b>3. REPORT TYPE AND DATES COVERED</b> Technical Memorandum	
<b>4. TITLE AND SUBTITLE</b> Microstructural Evolution of NARloy-Z at Elevated Temperatures		<b>5. FUNDING NUMBERS</b>	
<b>6. AUTHOR(S)</b> J. Singh, G. Jerman, B.N. Bhat, and R. Poorman			
<b>7. PERFORMING ORGANIZATION NAME(S) AND ADDRESS(ES)</b> George C. Marshall Space Flight Center Marshall Space Flight Center, Alabama 35812		<b>8. PERFORMING ORGANIZATION REPORT NUMBER</b>	
<b>9. SPONSORING / MONITORING AGENCY NAME(S) AND ADDRESS(ES)</b> National Aeronautics and Space Administration Washington, DC 20546		<b>10. SPONSORING / MONITORING AGENCY REPORT NUMBER</b>  NASA TM - 108419	
<b>11. SUPPLEMENTARY NOTES</b>  Prepared by Materials and Processes Laboratory, Science and Engineering Directorate.			
<b>12a. DISTRIBUTION / AVAILABILITY STATEMENT</b>  Unclassified—Unlimited		<b>12b. DISTRIBUTION CODE</b>	
<b>13. ABSTRACT (Maximum 200 words)</b>  Microstructural evolution was studied in samples of wrought and vacuum plasma sprayed (VPS) NARloy-Z exposed to temperatures up to 970 °C (1,780 °F) for up to 60 h. Samples were heated in a vacuum furnace, followed by rapid quenching in helium (He) gas at a cooling rate of ~166 °C (300 °F) per second. Microstructural analyses were conducted using optical microscopy, scanning electron microscopy (SEM), and electron probe microanalysis (EPMA). In both the wrought and VPS conditions, precipitates rich in silver (Ag) and zirconium (Zr) were present in the matrix and at the grain boundaries even after long exposure to elevated temperatures. Islands rich in oxygen (O <sub>2</sub> ) and Zr were also observed, as well as incipient melting at the grain boundary triple points. Results indicated that the alloy cannot be homogenized by heat treatment at elevated temperatures.			
<b>14. SUBJECT TERMS</b> VPS, SEM, EPMA, intermetallic precipitate, discontinuous precipitation, glazing, NARloy-Z			<b>15. NUMBER OF PAGES</b> 30
			<b>16. PRICE CODE</b> NTIS
<b>17. SECURITY CLASSIFICATION OF REPORT</b> Unclassified	<b>18. SECURITY CLASSIFICATION OF THIS PAGE</b> Unclassified	<b>19. SECURITY CLASSIFICATION OF ABSTRACT</b> Unclassified	<b>20. LIMITATION OF ABSTRACT</b> Unlimited

## TABLE OF CONTENTS

	Page
INTRODUCTION .....	1
BACKGROUND .....	1
A. NARloy-A .....	1
B. NARloy-Z and the Zr Addition.....	2
EXPERIMENTAL PROCEDURE .....	2
RESULTS AND DISCUSSION .....	3
A. Wrought NARloy-Z .....	3
B. VPS NARloy-Z.....	4
CONCLUSIONS.....	4
REFERENCES.....	6

PRECEDING PAGE BLANK NOT FILMED



## LIST OF ILLUSTRATIONS

Figure	Title	Page
1a.	SSME main combustion chamber.....	7
1b.	MCC schematic of cooling channel locations.....	8
2a.	Optical micrograph of MCC liner fabricated from wrought NARloy-Z, with uniform microstructure in the hot wall (region A) and channel lands (region B) .....	9
2b.	Optical micrograph showing the microstructure of the channel land (region B) and cold wall (region D).....	9
3.	Optical micrographs of microstructural changes in the hot wall (region A) after hot firing .....	10
4.	Schematic line diagram of the drop-through vacuum annealing and quenching furnace .....	11
5.	Optical and SEM micrographs of wrought NARloy-Z with precipitates at the grain boundaries and matrix.....	12
6a.	SEM-EDS analysis from one of the grain boundary precipitates, showing the presence of Zr-rich phases .....	13
6b.	EPMA analysis from one of the grain boundary precipitates, showing the presence of Ag- and Zr-rich phases .....	14
6c.	EPMA analysis from one of the matrix precipitates present in the wrought alloy showing the presence of Zr as an oxide ( $Zr_2O_3$ ) and the additional oxygen peak is due to the presence of $Cu_2O$ .....	15
7.	Optical micrographs of wrought NARloy-Z, in which islands have formed after exposure at 935 °C (1,715 °F) for up to 16 h (a) and 50 h (b).....	16
8.	Optical (a,b) and SEM (c,d) micrographs, showing islands after exposure at 935 °C (1,715 °F) for 50 h .....	17
9.	SEM-EDS spectra from figure 8, regions 1 to 4, with the composition of Ag- and Zr-rich phases present at the island grain boundaries .....	18
10.	EPMA across the matrix/island interface seen in figure 8a, regions A to B, with the composition profile and segregation of Zr and $O_2$ at the interface .....	19
11a.	Schematic line diagram of the sample showing different microstructure after elevated temperature exposure .....	20



## LIST OF ILLUSTRATIONS (continued)

Figure	Title	Page
11b.	Optical micrograph of the sample after exposure at 935 °C (1,715 °F) for 50 h (cross section is examined from the region as shown in fig. 11a), illustrating precipitate-free zone (region X).....	20
11c.	Optical micrograph of figure 11b from the region as marked by the arrow showing segregation of Zr-rich intermetallic phase at grain boundaries .....	20
12.	EPMA of regions A to B in figure 11a, with Ag concentration gradient from surface (A) to core (B) .....	21
13.	Optical (a) and SEM (b, c, d) micrographs after sample was exposed at 970 °C (1,780 °F) for 6 h, showing islands and incipient melting.....	22
14.	Optical micrographs (a, low magnification, and b, high magnification) of VPS NARloy-Z after exposure at 970 °C (1,780 °F) for 6 h, with grain boundary precipitates .....	23

## TECHNICAL MEMORANDUM

### MICROSTRUCTURAL EVOLUTION OF NARLOY-Z AT ELEVATED TEMPERATURES

#### INTRODUCTION

At present, the space shuttle main engine (SSME) main combustion chamber (MCC) liner is fabricated from wrought NARloy-Z (figs. 1a and 1b). Figure 2 shows that the liner consists of (A) a hot wall, (B) channel lands, and (C) cooling channels. The thickness of the hot wall varies from 0.5 to 0.75 mm (20 to 30 mils). Currently, the liner undergoes a heat treatment cycle that includes solutionization in a vacuum furnace at 935 °C (1,715 °F) for 4 h, water quenching to room temperature, and age hardening at 480 °C (900 °F) for 4 h. The cycle results in a homogeneous fine-grained microstructure with a uniform distribution of Cu-Ag-Zr intermetallic and Zr oxides in the matrix (fig. 2, regions A and B).

During hot firing, the hot wall is exposed to temperatures from -252 to >538 °C (-422 to >1,000 °F). This elevated temperature exposure causes microstructural changes that include precipitation and coarsening of intermetallic phases in the matrix and grain boundaries (fig. 3). At temperatures exceeding 538 °C (1,000 °F), such inhomogeneities tend to lower mechanical properties, especially ductility. This in turn leads to crack initiation (arrow, fig. 3), and ultimately to cracking of the hot wall (fig. 3a).

Efforts are underway to reduce the cost of MCC fabrication by using alternative processes such as vacuum plasma spraying (VPS). However, VPS NARloy-Z has an inhomogeneous microstructure with coarse precipitates in the matrix and at the grain boundaries. This study addresses the question of whether exposure to elevated temperatures will homogenize the VPS alloy to obtain a microstructure typical of the wrought alloy. The focus was placed on microstructural changes in wrought and VPS NARloy-Z after exposure to various elevated temperatures which were close to, yet below, the alloy melting point.

#### BACKGROUND

An understanding of the physical metallurgy of NARloy-A is necessary to understand NARloy-Z, especially the role of the Zr addition. NARloy-Z is a ternary alloy (Cu-3 wt.% Ag-0.5 wt.% Zr) derived from the binary alloy NARloy-A (Cu-3 wt.% Ag).

##### A. NARloy-A

NARloy-A undergoes quite complex decomposition reactions. Ag-rich phases experience continuous/discontinuous precipitation during aging at 480 °C (900 °F) for 4 h. Continuous precipitation can take place before, during, or after discontinuous precipitation.<sup>1</sup>

Continuous precipitation is responsible for age hardening of the alloy and occurs when an Ag-rich phase is uniformly distributed into the matrix. These precipitates have the same orientation as the matrix, but a slightly different lattice parameter, making them semicoherent.



Discontinuous precipitation refers to selective grain boundary precipitation. This condition results in a eutectic-like structure that reduces the mechanical properties of NARloy-A.

### B. NARloy-Z and the Zr Addition

Reports indicate that discontinuous precipitation is inhibited when Zr is added to Cu-3 wt.% Ag. The presence of Zr makes three major contributions to the microstructure of NARloy-Z:<sup>2</sup>

1. Grain growth is restricted by pinning Cu grain boundaries with Cu-Ag-Zr intermetallic compounds.
2. Discontinuous precipitation is inhibited by Zr, which promotes homogeneous precipitation of Ag-rich phases on aging.
3. Zr deoxidizes the alloy and removes Cu<sub>2</sub>O from the grain boundaries, improving ductility at elevated temperatures.

Based on the binary phase diagrams, the maximum solid solubility of Zr in the Cu matrix is about 0.1 wt.% at 935 °C (1,715 °F). Since NARloy-Z only contains about 0.5 wt.% Zr, the excess will precipitate either as a Zr-rich intermetallic phase or as Zr oxide (Zr<sub>2</sub>O<sub>3</sub>).

To achieve the best thermal conductivity and mechanical properties, the recommended heat treatment cycle for wrought NARloy-Z is to solutionize at 935 °C (1,715 °F) for 4 h, water quench, and then age at 480 °C (900 °F) for 4 h. The Ag-rich phase will uniformly precipitate out, giving an age hardening effect.

Wrought NARloy-Z contains traces of O<sub>2</sub> (~50 ppm). Zr is assumed to absorb any O<sub>2</sub> present in the matrix, forming stable Zr oxide which is uniformly dispersed throughout the matrix. The Ag-rich phase is assumed to provide precipitation hardening during the heat treatments discussed above. However, formation of complex Zr- and Ag-rich intermetallic phases and their influence on the microstructure and mechanical properties are not well understood.

In an MCC liner fabricated from VPS NARloy-Z, the microstructure showed large volume fractions of undesirable grain boundary precipitates, cavities, etc. The relatively high O<sub>2</sub> content (200 to 500 ppm) segregated to the grain boundaries as Zr and Cu oxides during the deposition process. As a result, microstructural inhomogeneity contributed to lower mechanical properties in VPS NARloy-Z.<sup>3 4</sup>

### EXPERIMENTAL PROCEDURE

The present investigation used samples of wrought and VPS NARloy-Z, containing precipitates of Ag- and Zr-rich phases in the matrix. Prior heat treatment histories were as follows:

1. The wrought material was centrifugally cast, hot rolled into shape, and then heated in a vacuum furnace to 935 °C (1,715 °F) for 4 h, followed by a water quench. The material was heated again in a vacuum furnace to 537 °C (1,000 °F) for 8 h, followed by a second water quench.



2. The VPS material was sprayed at 870 °C (1,600 °F) for 4 h, slow cooled, and then hot isostatically pressed at 870 °C (1,600 °F) for 2 h at 15 ksi.

All samples were heated in a drop-through vacuum furnace (fig. 4) to temperatures ranging from 935 to 970 °C (1,715 to 1,780 °F) for up to 50 h, then rapidly quenched by He gas.

Metallographic samples were prepared and etched using an ammonium persulfate solution ((NH<sub>4</sub>)<sub>2</sub>S<sub>2</sub>O<sub>8</sub> per 100 mL H<sub>2</sub>O). The samples were examined with an optical microscope, a Hitachi S-4000 field emission scanning electron microscope (SEM), and a Cameca SX-50 electron microprobe. Elemental analysis of different phases was performed using qualitative energy dispersive spectroscopy (EDS) and electron probe microanalysis (EPMA).

## RESULTS AND DISCUSSION

### A. Wrought NARloy-Z

Optical and SEM micrographs for heat-treated wrought NARloy-Z are shown in figure 5. Both Ag- and Zr-rich intermetallic phases were present in the Cu matrix and grain boundaries. Figure 6a shows a typical EDS spectrum of the Zr-rich intermetallic phase at the grain boundary (arrows in fig. 5). Zr oxide was also present, probably as Zr<sub>2</sub>O<sub>3</sub> in the matrix. An EPMA was used to determine the concentration profile across the intermetallic phase (fig. 6b). Oxygen was present probably as Cu<sub>2</sub>O (fig. 6b) and also as Zr<sub>2</sub>O<sub>3</sub> (fig. 6c).

After heating to 935 °C (1,715 °F) for 16 h, the surface still contained undissolved precipitates and islands (fig. 7). The islands were 200 to 400 μm in size and had a volume fraction of approximately 30 percent. Figure 8 indicates that the islands persisted when the same sample was heated again for 50 h at 935 °C (1,715 °F). The grain size within the islands (~50 μm) was relatively small compared to the grain size in the matrix (~200 μm). Intermetallic Ag- and Zr-rich precipitates were also observed in the matrix and at the grain boundaries of the islands. Figure 9 shows EDS analysis of different precipitates (marked 1 and 2), indicating that each precipitate had a different chemistry. The composition of the matrix phase is about the same within and outside the island (areas 4 and 3, respectively, figs. 8 and 9). The concentration gradient of each alloying element in the bulk material (region A, fig. 8a) and the island (region B, fig. 8a) is given in an EPMA (fig. 10). Negligible amounts of Zr and O<sub>2</sub> were observed in region A, as compared to region B (fig. 10). The Zr and O<sub>2</sub> concentrations peaked at the matrix/island interface. They decreased as a function of diffusion distance within the island, although region B contained high average concentrations (about 0.8 and 0.3 wt.%, respectively). These concentrations increased at island grain boundaries (probably due to the formation of stable Zr oxide at the A/B interface) and were higher within the island. The average grain size in region A was about three times larger than in region B. The cause of migration of Zr and O<sub>2</sub> from the bulk and segregation at grain boundaries, forming islands, is unknown. Ag loss from the surface probably occurred during heat treatment, due to higher partial pressure of Ag vapor in the furnace, as compared with Cu and Zr. However, the Ag concentration averaged about 1.7 wt.% throughout the surface of regions A and B.

A cross section of this sample was examined to determine the Ag concentration gradient and depth of loss. In figure 11, optical micrographs reveal an almost precipitate-free zone near the surface



(region X) and still undissolved intermetallic precipitates in the bulk (region Y). The average grain size in region X (200 to 300  $\mu\text{m}$ ) was about twice that seen in the core (70 to 100  $\mu\text{m}$ ).

Figure 12 shows the Ag concentration gradient across region AB of figure 11b. About 0.3 wt.% Ag was observed at the surface of depleted region X, increasing linearly as a function of diffusion distance towards the core (region Y) and leveling off at about 3.3 wt.%. Zr and  $\text{O}_2$  concentrations were negligible in region X and increased towards region Y as a function of diffusion distance.

Island formation and the persistence of intermetallic phases were confirmed by another sample, heated to 970  $^{\circ}\text{C}$  (1,780  $^{\circ}\text{F}$ ) for 6 h. Undissolved second phases, islands, and incipient melting of grain boundary triple points were observed on the surface (see arrows in fig. 13). The results indicate that intermetallic Cu-Ag-Zr phases are difficult to redissolve, even when the sample is heated close to the melting point.

During elevated temperature exposure, two types of microstructural phenomena apparently occurred: (1) grain growth at the surface and (2) migration and coarsening of undissolved Zr and intermetallic phases. The combined effect of grain boundary diffusion and grain growth led to grain boundary segregation of Zr and intermetallic phases. Since Zr has more affinity for  $\text{O}_2$  than Cu and Ag, traces of  $\text{O}_2$  present in the matrix migrated with Zr to form stable  $\text{Zr}_2\text{O}_3$ .

## B. VPS NARloy-Z

Prior to heat treatment, the VPS NARloy-Z samples had a two-phase microstructure, composed of a matrix and grain boundary precipitates. The average grain size was about 30  $\mu\text{m}$ , which was smaller than that of the wrought alloy ( $\sim 100$   $\mu\text{m}$ ). Although these samples were heated to 970  $^{\circ}\text{C}$  (1,780  $^{\circ}\text{F}$ ) for 6 h and rapidly quenched with He gas, optical micrographs showed that the grain boundary precipitates did not redissolve into the matrix (fig. 14). Even prolonged exposure to elevated temperatures did not appear to produce any change in the microstructure, and no grain growth was observed.

Wrought and VPS NARloy-Z had very similar compositions, but their microstructures were quite different in areas such as grain size, volume fraction, size and distribution of intermetallic phases, and presence of Zr oxides. These variations probably resulted from different processing conditions. However, the samples continued to have different microstructures even after both were exposed to an elevated temperature of 970  $^{\circ}\text{C}$  (1,780  $^{\circ}\text{F}$ ). Such behavior is different from steels or Ni-based alloys, in which a single phase can generally be obtained after a suitable elevated temperature solution treatment.

Other techniques may be more effective for homogenizing NARloy-Z. A recent investigation demonstrated that microstructural inhomogeneity (such as grain boundary precipitation, voids, and cavities) in wrought and VPS NARloy-Z can be eliminated using a process called "glazing," which creates a uniform microstructure by rapidly melting and resolidifying the surface with high energy electron or laser beams. This research will be published elsewhere.<sup>5</sup>

## SUMMARY

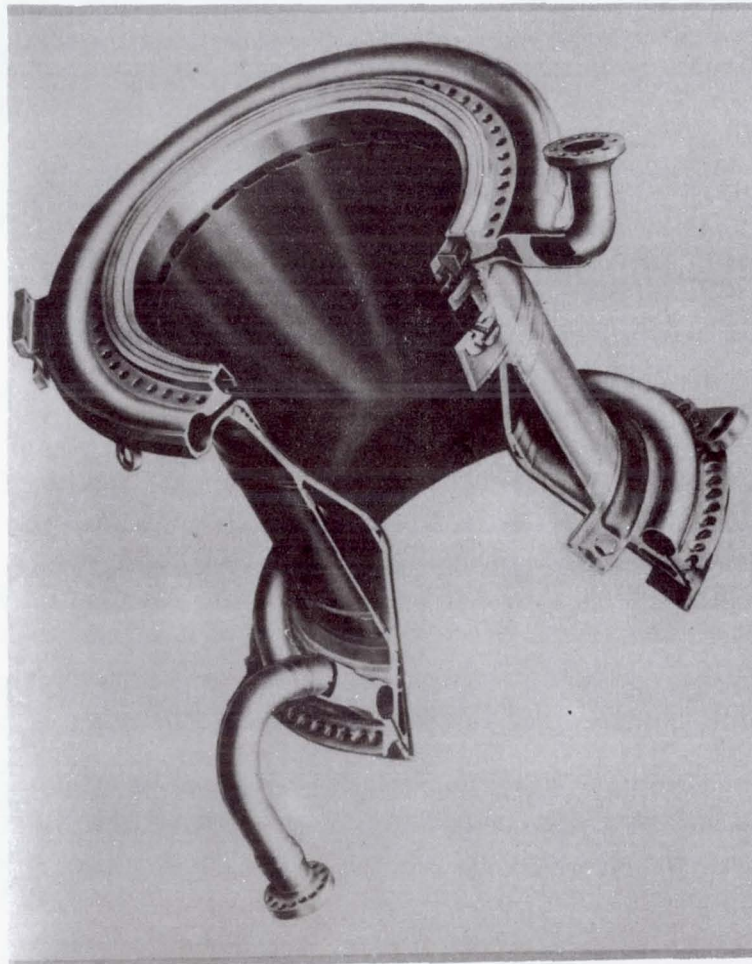
Homogenization treatment at elevated temperatures up to 970  $^{\circ}\text{C}$  (1,780  $^{\circ}\text{F}$ ) was conducted for up to 60 h on samples of wrought and VPS NARloy-Z. The samples had the same composition, but

different processing histories and initial microstructures. Grain growth was observed during homogenization. Excess Zr and O<sub>2</sub> segregated at the grain boundaries, forming Zr<sub>2</sub>O<sub>3</sub> and intermetallic compounds of Cu-Ag-Zr. In wrought NARloy-Z, islands approximately 200 μm in diameter were formed, with Zr- and O<sub>2</sub>-rich elements in the matrix and at the grain boundaries. Their volume fraction was ~30 percent. In both cases, the intermetallic Ag- and Zr-rich phases precipitated out (e.g., in service or during VPS or thermomechanical treatments), and they could not be redissolved into the matrix by solutionizing at elevated temperatures.



## REFERENCES

1. Singh, J., and Suryanarayana, C.: *Journal of Materials Science*, vol. 27, 1992, p. 4261.
2. Paton, N.E. and Robertson, W.M.: "Metallurgy of NARloy-Z." Rocketdyne Technical Progress Report, March 1973.
3. Sanders, J.H.: "Investigation of Main Combustion Chamber Liner 4011 Degradation." IIT Research Institute/MRF Report P06150-P495B, January 1992.
4. Chen, P.S.: "An Investigation on the Ductility Loss of VPS NARloy-Z at Elevated Temperatures." IIT Research Institute/MRF Report P06150-P499, August 1992.
5. Singh, J., Jerman, G., Bhat, B.N., and Poorman, R.: "Microstructural Study in Wrought, Laser, and Electron Beams Glazed NARloy-Z." NASA Technical Report, under preparation, 1993.



### GEOMETRY

■ NARLOY Z LINER + EDCu BARRIER + EDNi CLOSE-OUT + INCO 718 STRUCTURE SHELL	
■ NUMBER OF SLOTS	390
■ NUMBER OF ACOUSTIC CAVITIES	30
■ INJECTOR END DIAMETER	17.74 IN.
■ THROAT AREA	83.41 IN. <sup>2</sup>
■ INJECTOR END TO THROAT LENGTH	14.00 IN.
■ CONTRACTION RATIO	2.96:1
■ EXPANSION RATIO	5.0:1

### OPERATING PARAMETERS (RPL, MR-6.0)

■ THROAT STAGNATION PRESSURE	3009 PSIA
■ COOLANT INLET PRESSURE	5949 PSIA
■ COOLANT INLET TEMPERATURE	96 R
■ COOLANT EXIT PRESSURE	4543 PSIA
■ COOLANT EXIT TEMPERATURE	477 R
■ COOLANT FLOWRATE	26.75 LB/SEC
■ HOT GAS WALL TEMPERATURE AT THROAT	1000 F

Figure 1a. SSME main combustion chamber.

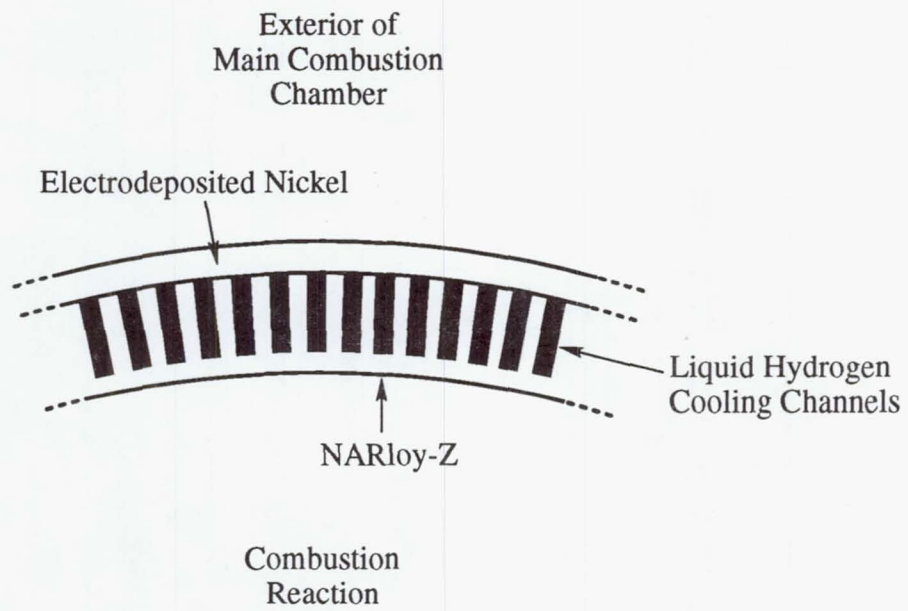
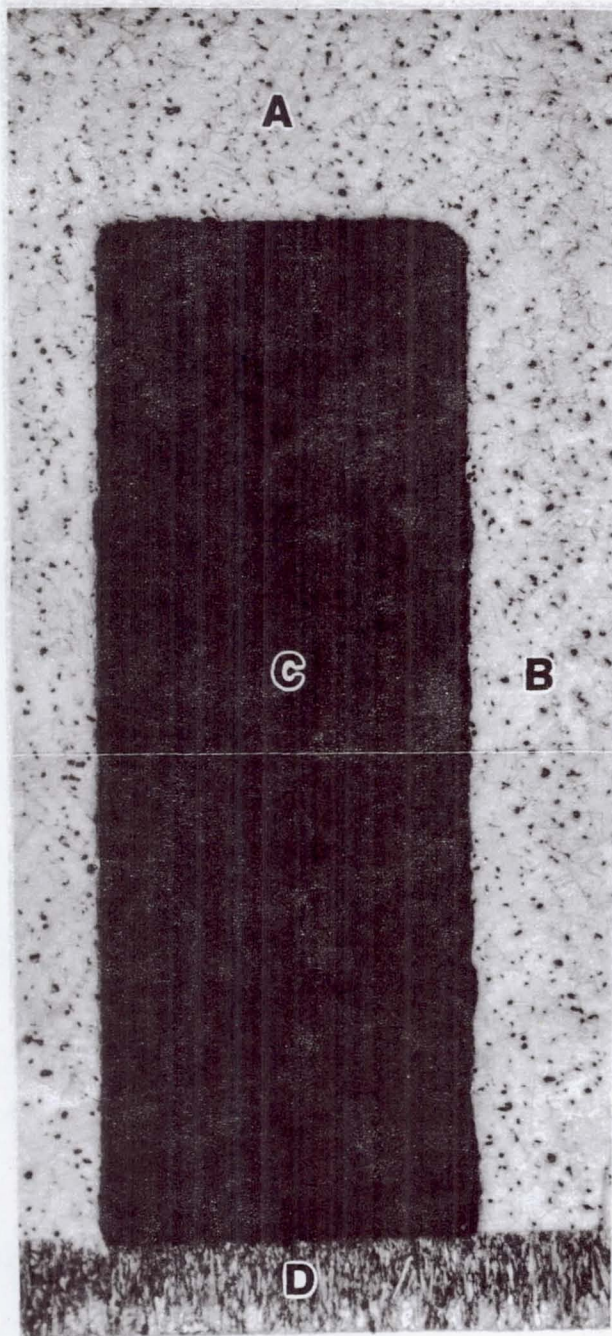


Figure 1b. MCC schematic of cooling channel locations.

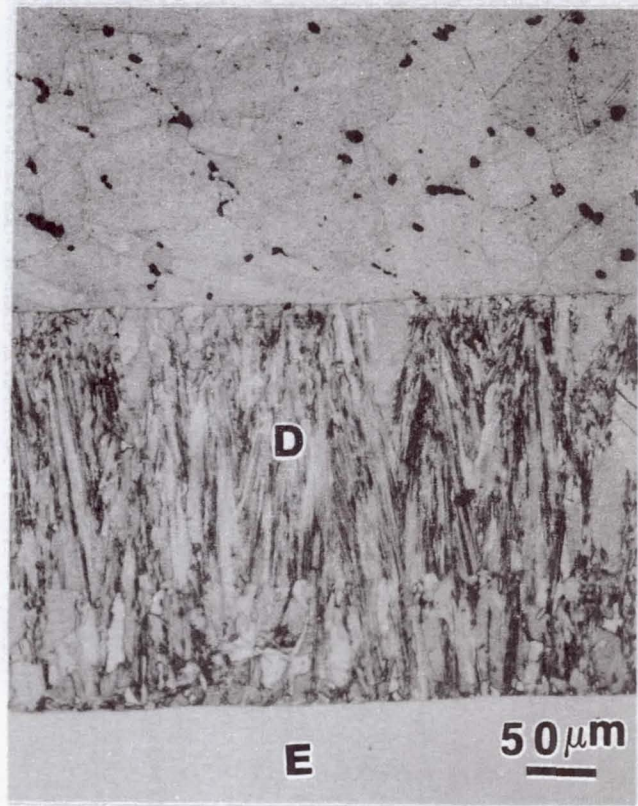




E

200  $\mu\text{m}$

Figure 2a. Optical micrograph of MCC liner fabricated from wrought NARloy-Z, with uniform microstructure in the hot wall (region A) and channel lands (region B).



D

E

50  $\mu\text{m}$

- A – Hot wall
- B – Channel land
- C – Cooling channels
- D – Cold wall (ED Cu)
- E – Electrodeposited Ni

Figure 2b. Optical micrograph showing the microstructure of the channel land (region B) and cold wall (region D).

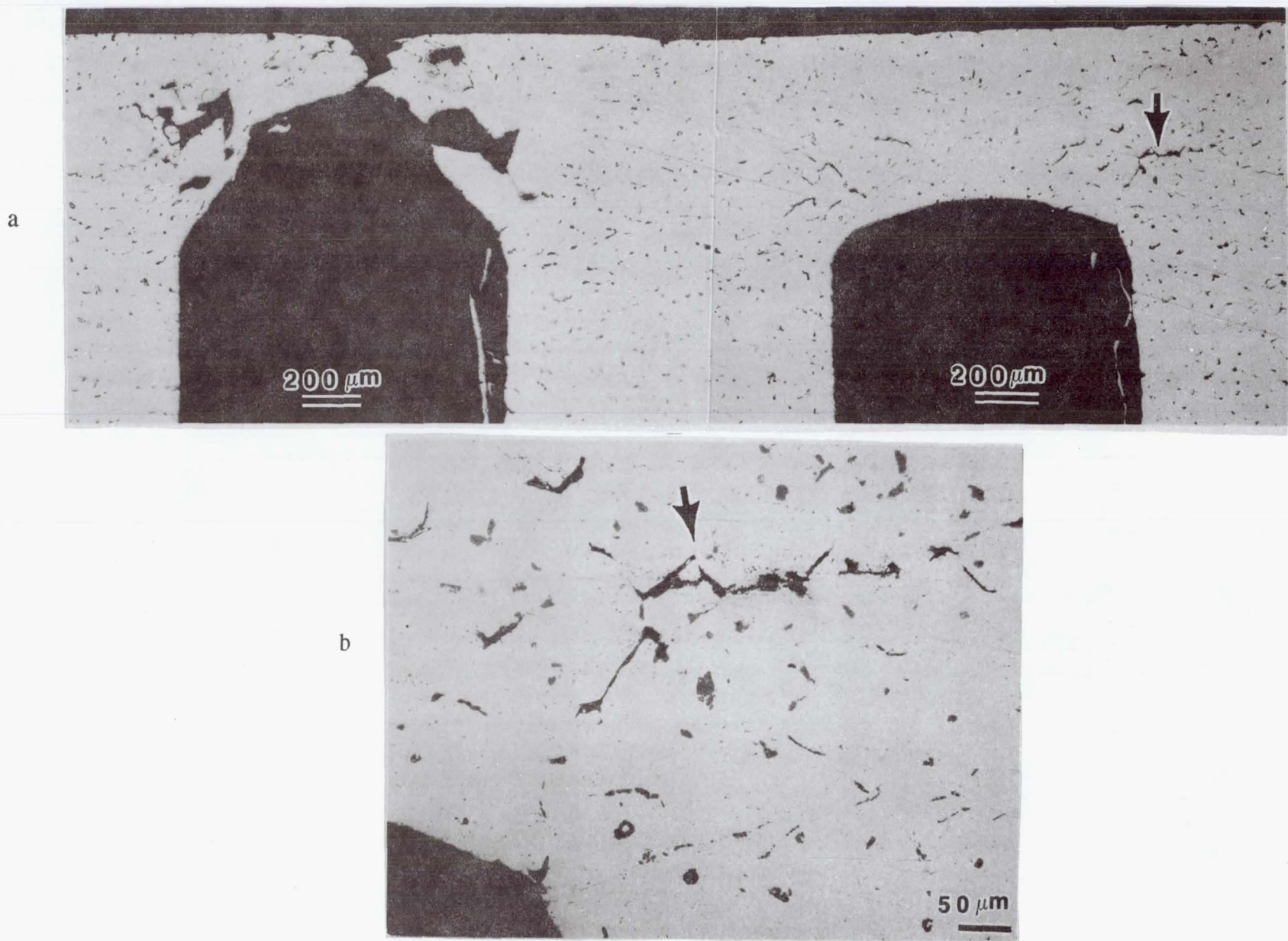


Figure 3. Optical micrographs of microstructural changes in the hot wall (region A) after hot firing.



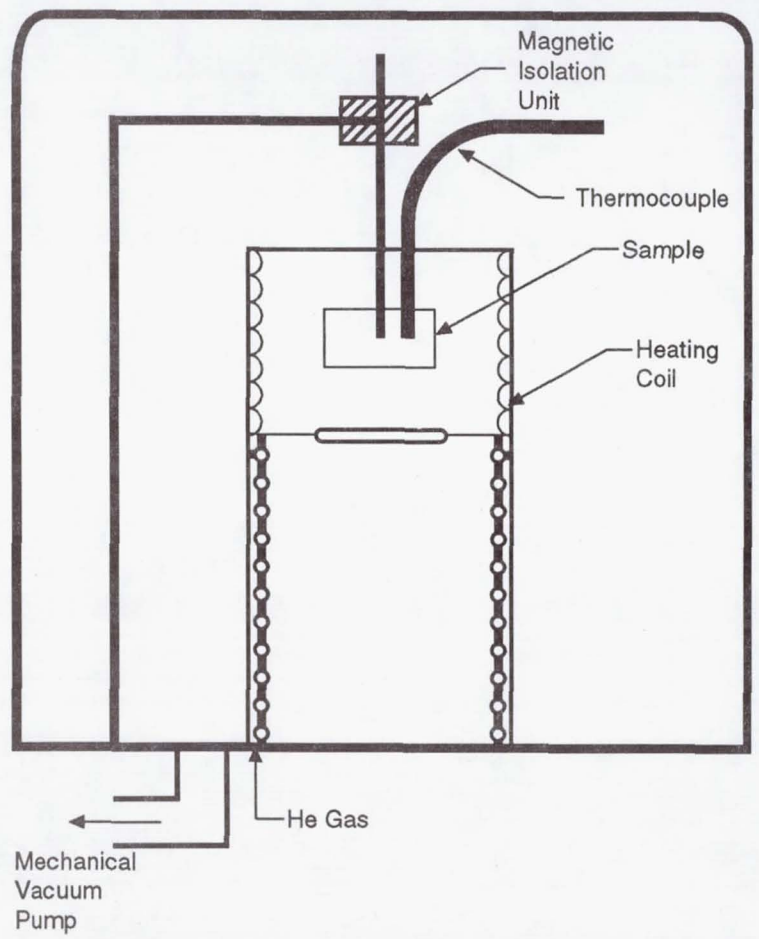


Figure 4. Schematic line diagram of the drop-through vacuum annealing and quenching furnace.



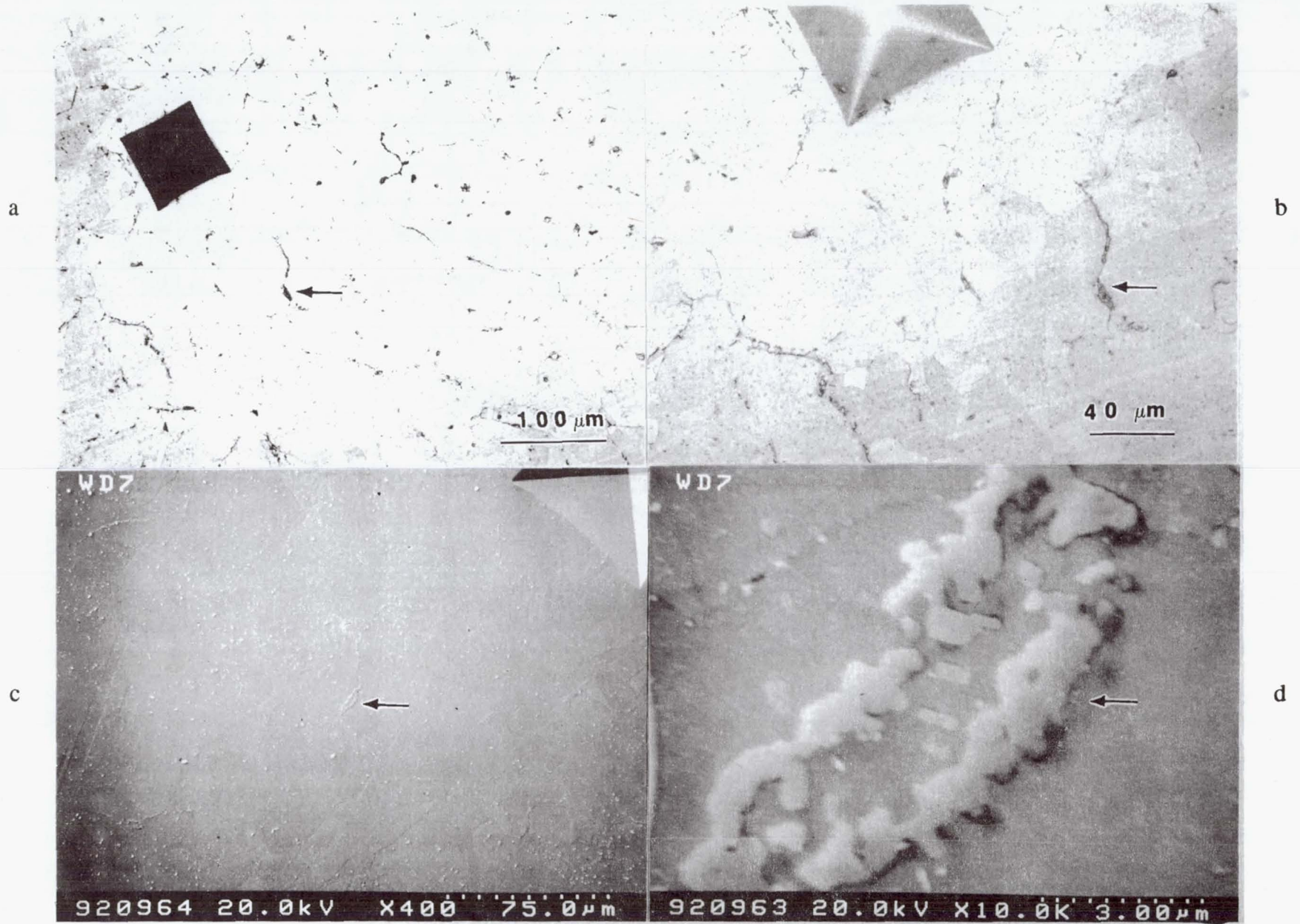


Figure 5. Optical (a and b) and SEM (c and d) micrographs of wrought NARloy-Z with precipitates at the grain boundaries and matrix. Arrow represents same area.

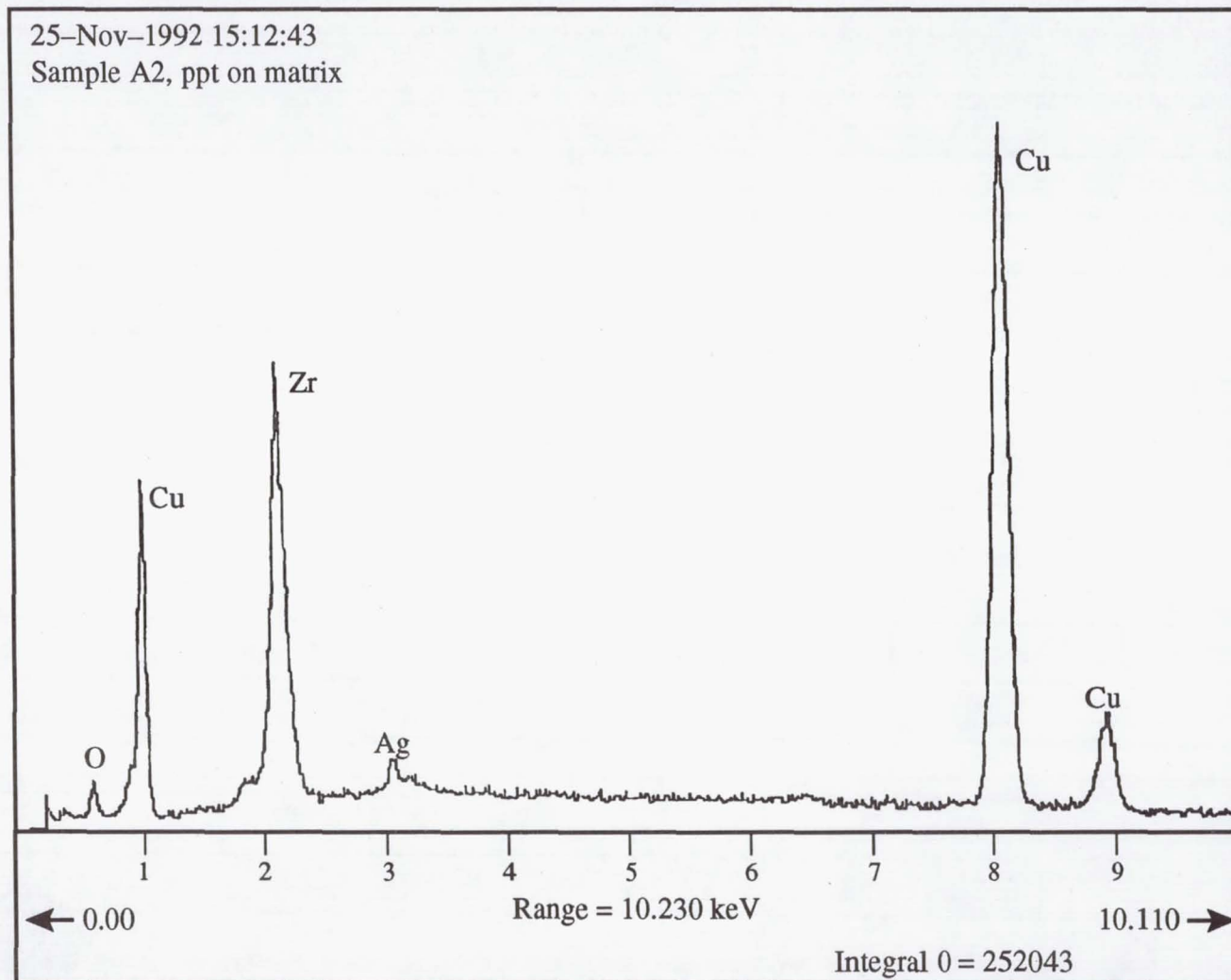


Figure 6a. SEM-EDS analysis from one of the grain boundary precipitates, showing the presence of Zr-rich phases.

From Intermetallic Phase  
 Camebax-SX- Beam scanning  
 Vertical Linear scale

SP1: O    Max: 2082    Vertical scale: 140 counts/cm  
 SP2: Ag    Max: 2918    Vertical scale: 200 counts/cm  
 SP3: Zr    Max: 3756    Vertical scale: 250 counts/cm

Beam Current: 14.96 nA  
 High Voltage: 20.00 kV  
 Counting Time: 10,000 mS

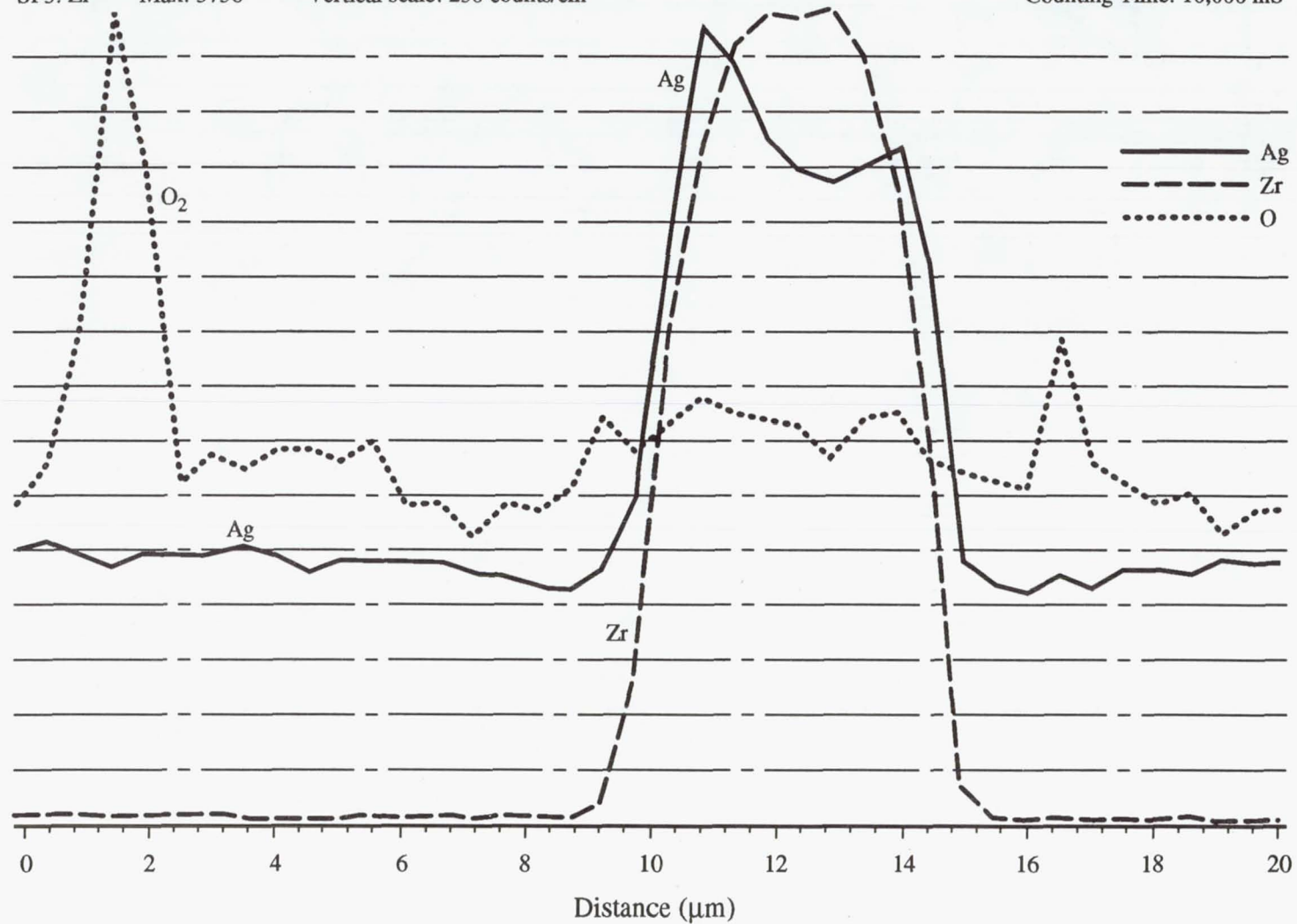


Figure 6b. EPMA analysis from one of the grain boundary precipitates, showing the presence of Ag- and Zr-rich phases.



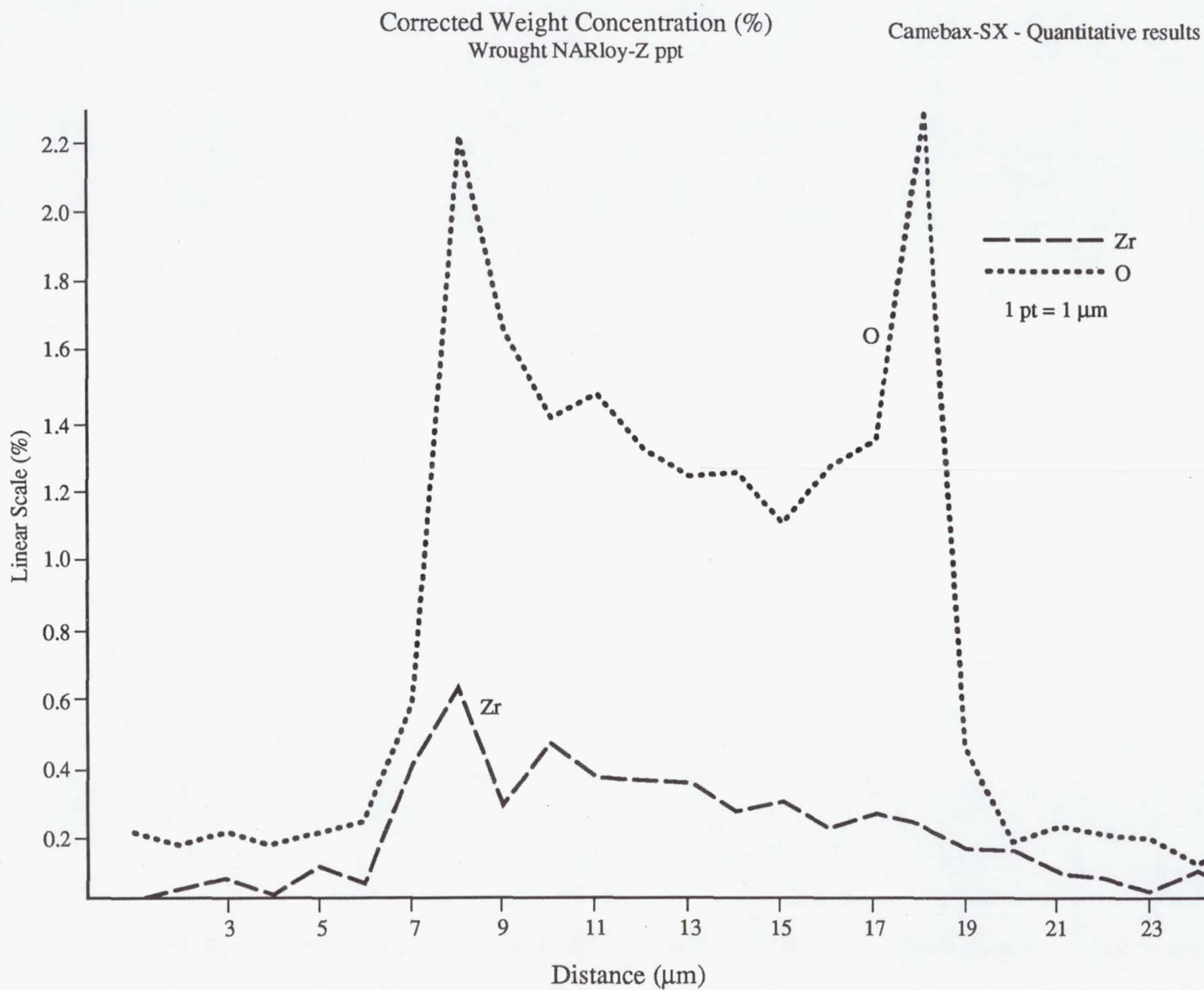


Figure 6c. EPMA analysis from one of the matrix precipitates present in the wrought alloy showing the presence of Zr as an oxide ( $\text{Zr}_2\text{O}_3$ ) and the additional oxygen peak is due to the presence of  $\text{Cu}_2\text{O}$ .

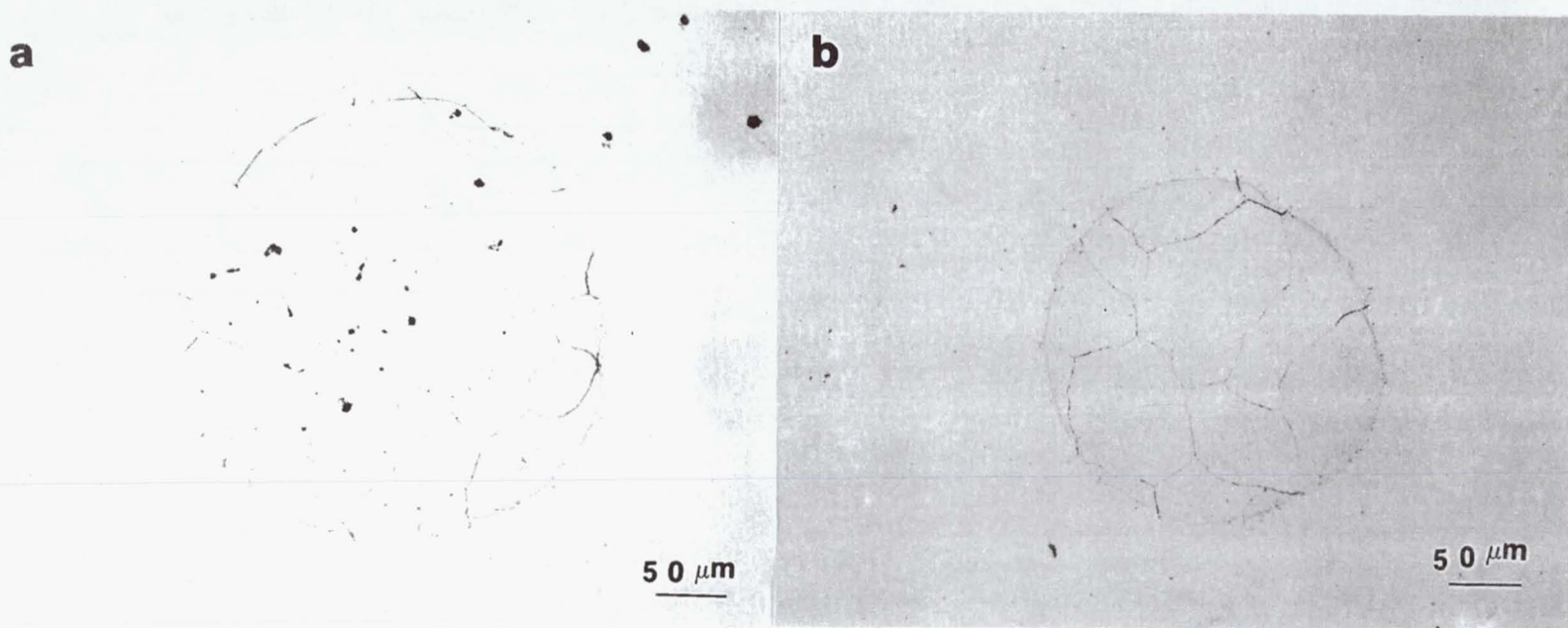


Figure 7. Optical micrographs of wrought NARloy-Z, in which islands have formed after exposure at 935 °C (1,715 °F) for up to 16 h (a) and 50 h (b).



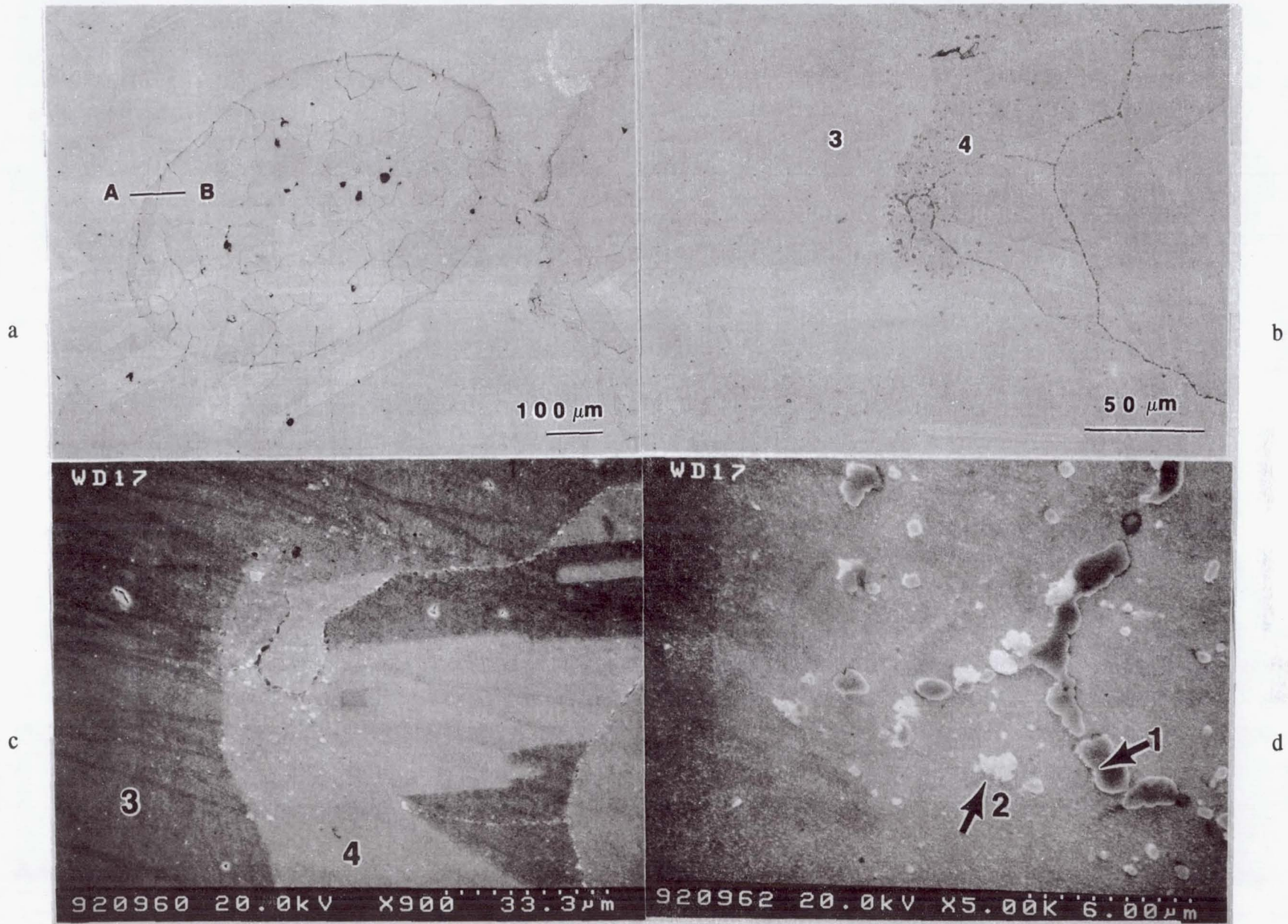


Figure 8. Optical (a,b) and SEM (c,d) micrographs, showing islands after exposure at 935 °C (1,715 °F) for 50 h.

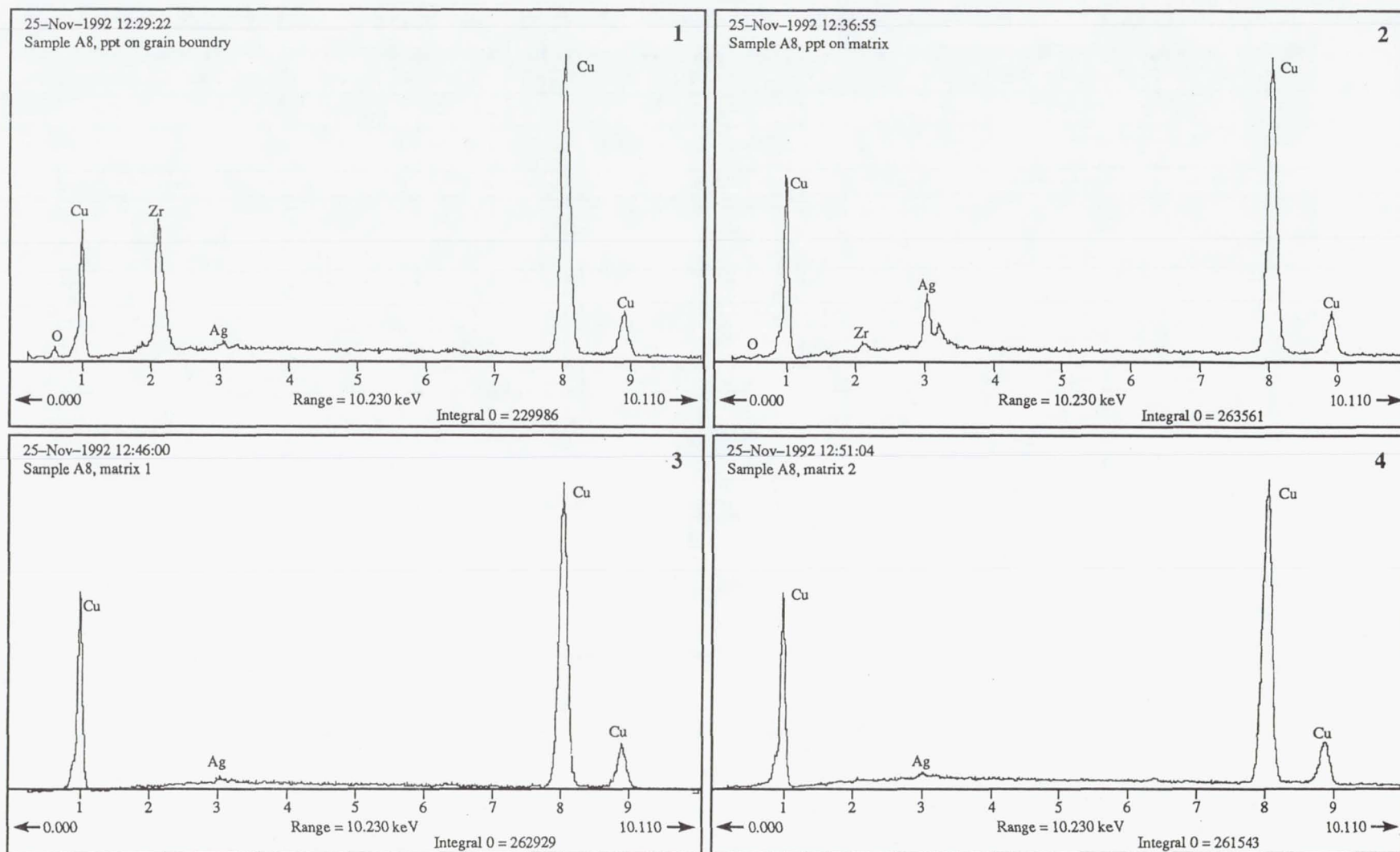


Figure 9. SEM-EDS spectra from figure 8, regions 1 to 4, with the composition of Ag- and Zr-rich phases present at the island grain boundaries.



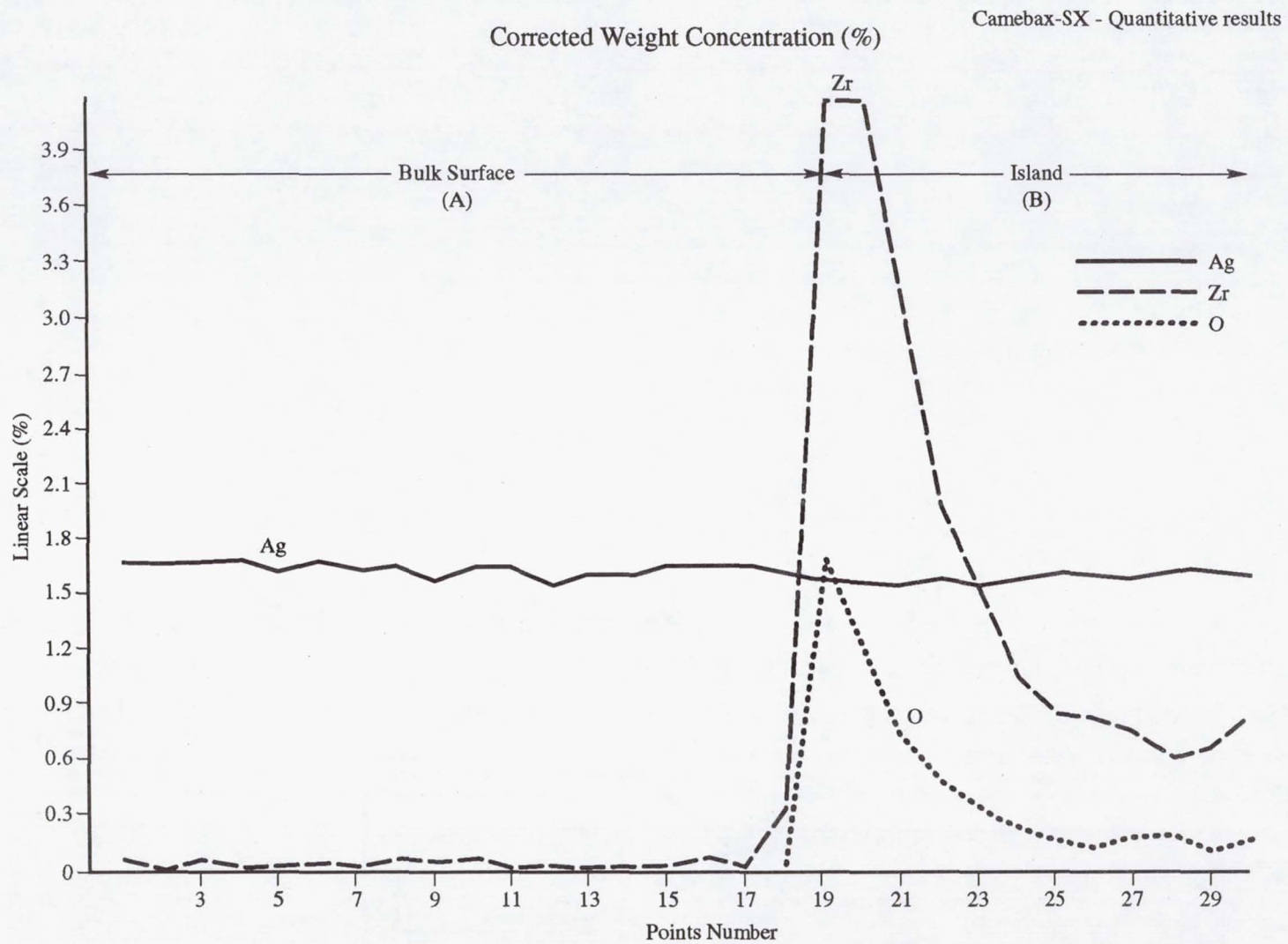


Figure 10. EPMA across the matrix/island interface seen in figure 8a, regions A to B, with the composition profile and segregation of Zr and O<sub>2</sub> at the interface.

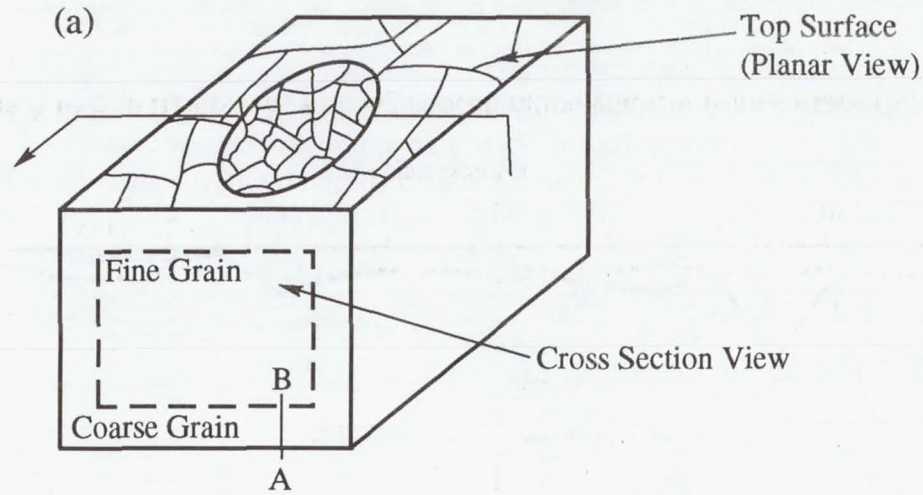


Figure 11a. Schematic line diagram of the sample showing different microstructures after elevated temperature exposure.

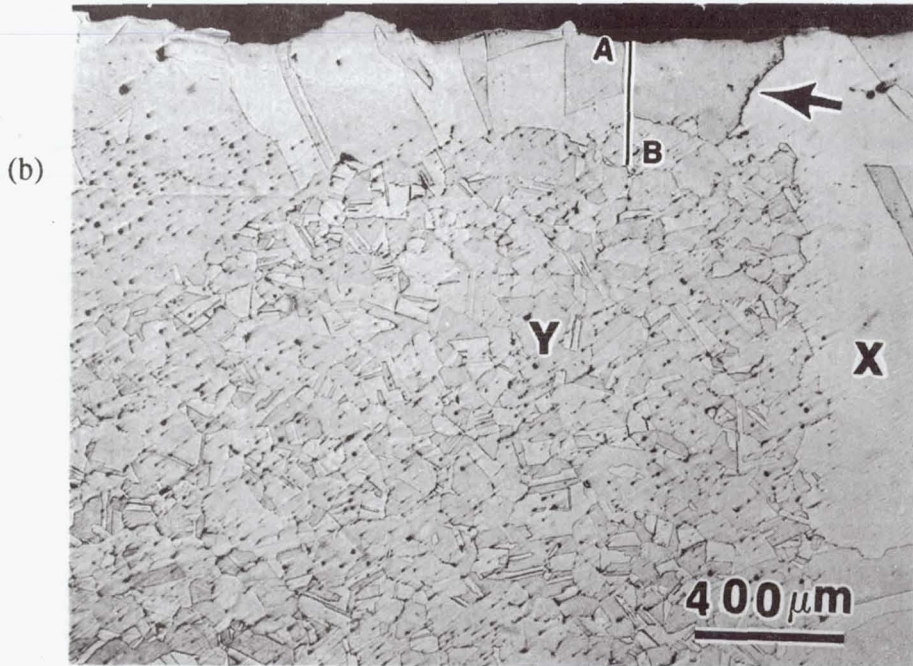


Figure 11b. Optical micrograph of the sample after exposure at 935 °C (1,715 °F) for 50 h (cross section is examined from the region as shown in fig. 11a), illustrating precipitate-free zone (region X).

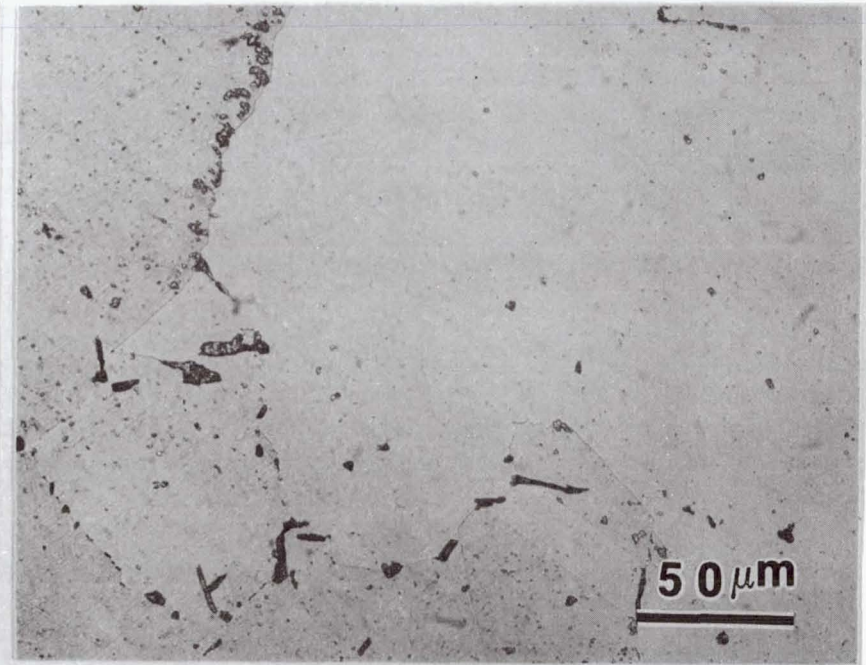


Figure 11c. Optical micrograph of figure 11b from the region as marked by the arrow showing segregation of Zr-rich intermetallic phase at grain boundaries.



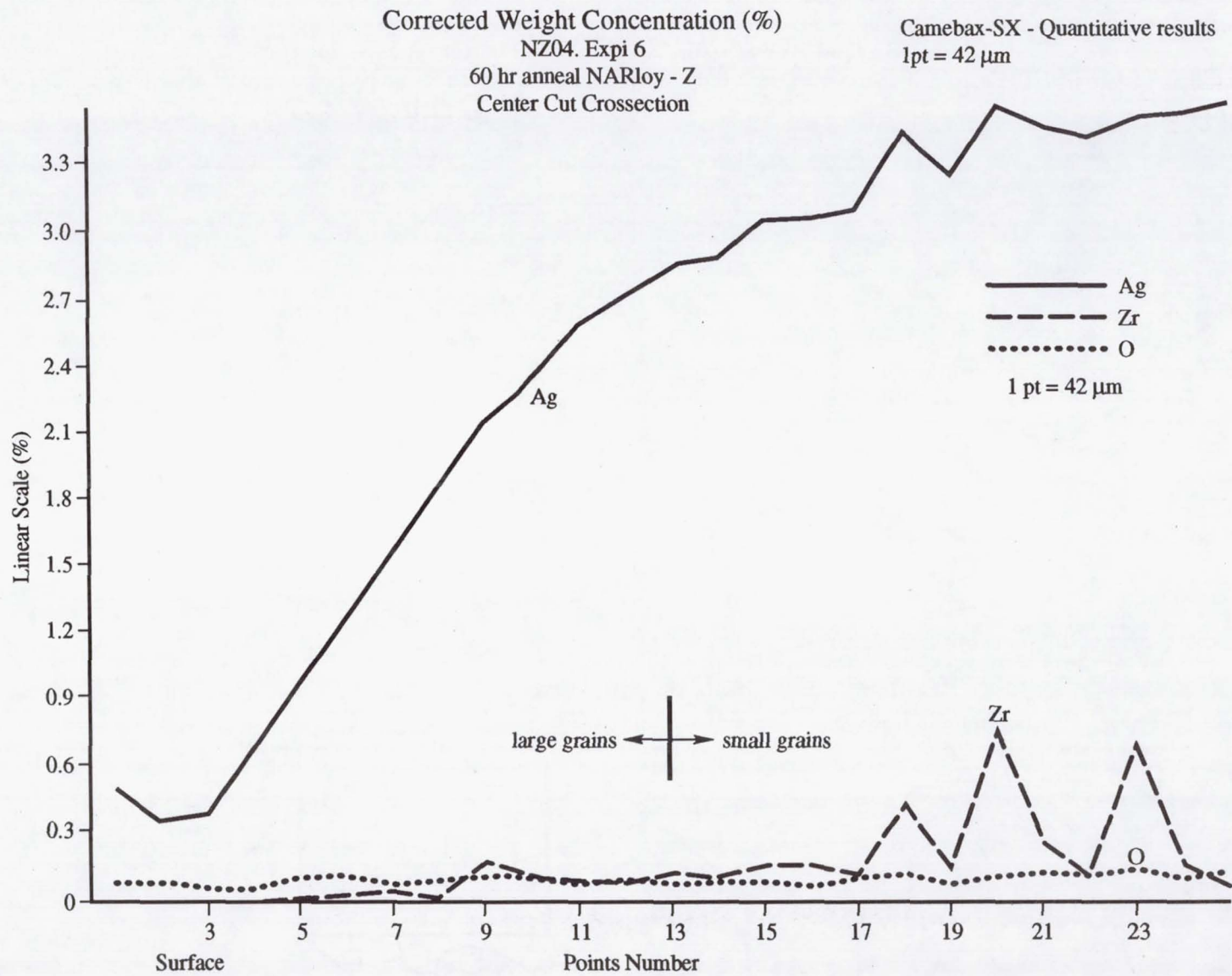
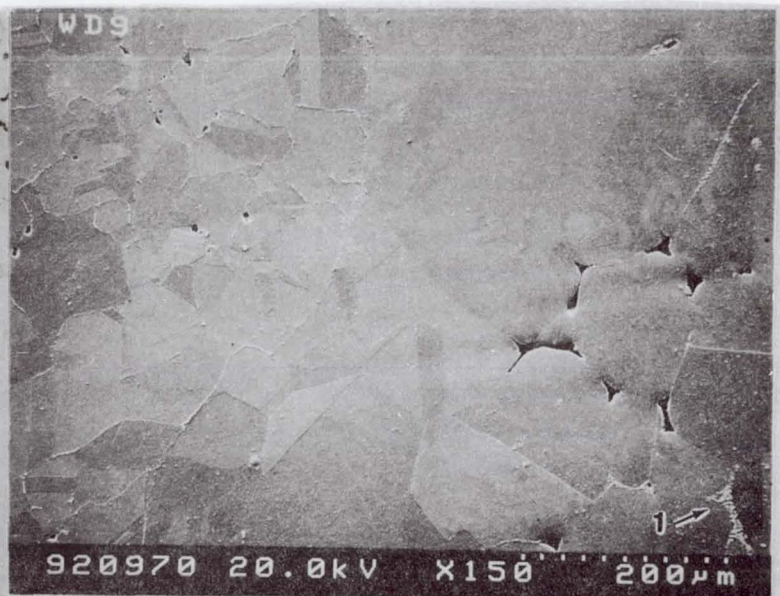


Figure 12. EPMA of regions A to B in figure 11a, with Ag concentration gradient from surface (X) to core (Y) in figure 11b.

a



b



c



d



Figure 13. Optical (a) and SEM (b, c, d) micrographs after sample was exposed at 970 °C (1,780 °F) for 6 h, showing islands and incipient melting. Arrows represent same area.



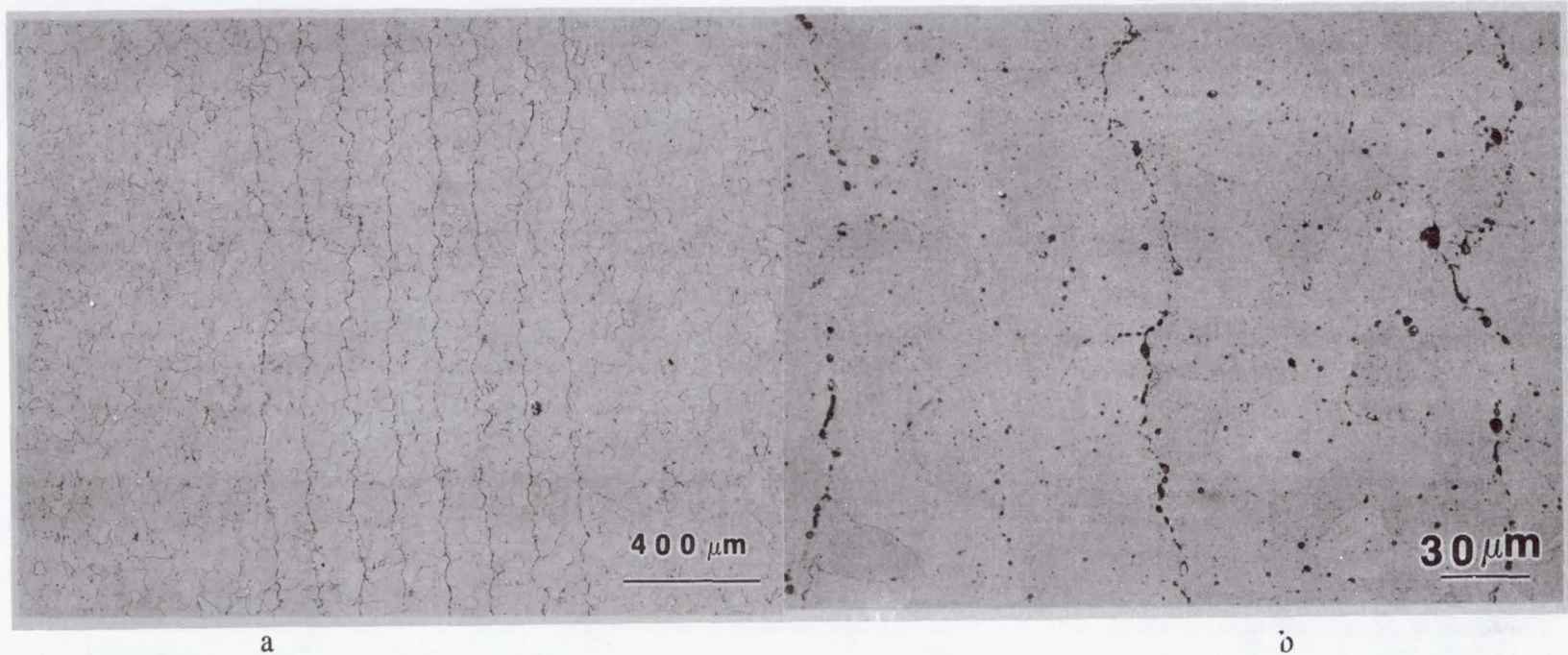


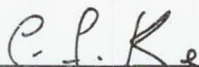
Figure 14. Optical micrographs (a, low magnification, and b, high magnification) of VPS NARloy-Z after exposure at 970 °C (1,780 °F) for 6 h, with grain boundary precipitates.

## APPROVAL

### MICROSTRUCTURAL EVOLUTION OF NARLOY-Z AT ELEVATED TEMPERATURES

By J. Singh, G. Jerman, B.N. Bhat, and R. Poorman

The information in this report has been reviewed for technical content. Review of any information concerning Department of Defense or nuclear energy activities or programs has been made by the MSFC Security Classification Officer. This report, in its entirety, has been determined to be unclassified.



---

P.H. SCHUERER  
Director, Materials and Processes Laboratory